Available online at www.sciencedirect.com
SCIENCE DIRECT®
Optics Communications 259 (2006) 474–478
OPTICS COMMUNICATIONS
www.elsevier.com/locate/optcom

Effects of the frequency chirp on the fields of a chirped Gaussian pulse passing through a hard-edged aperture

Runwu Peng [a,b,*], Zhixiang Tang [a,b], Yunxia Ye [b,c], Shuangchun Wen [a], Dianyuan Fan [b]

[a] School of Computer and Communication, Hunan University, Changsha 410082, China
[b] Shanghai Institute of Optics and Fine Mechanics, Chinese Academy of Sciences, P.O. Box 800-211, Shanghai 201800, China
[c] Mechanical Engineering College, Jiangsu University, Zhenjiang 212013, China

Received 28 June 2005; received in revised form 7 September 2005; accepted 20 September 2005

Abstract

Based on the Huygens–Fresnel diffraction integral and Fourier transform, propagation expression of a chirped Gaussian pulse passing through a hard-edged aperture is derived. Intensity distributions of the pulse with different frequency chirp in the near-field and far-field are analyzed in detail by numerical calculations. In the near-field, amplitudes of the intensity peaks generated by the modulation of the hard-edged aperture decrease with increasing the frequency chirp, which results in the improving of the beam uniformity. A physical explanation for the smoothing effect brought by increasing the frequency chirp is given. The smoothing effect is achieved not only in the pulse with Gaussian transverse profile but also in the pulse with Hermite–Gaussian transverse profile when the frequency chirp increases.

PACS: 42.25.Bs; 42.25.Fx; 42.60.Jf; 42.79.Ag

Keywords: Frequency chirp; Broadband laser; Beam smoothing; Hard-edged aperture

1. Introduction

Hard-edged aperture is a general optical element in optical systems. When a laser pulse passes through a hard-edged aperture, non-uniform intensity is generated, which is a disadvantage for the applications of laser. In the inertial confinement fusion, non-uniform intensity imprints itself on the target causing surface damage, which can "seed" the Rayleight–Taylor fluid instability, and enhances the ignition energy [1,2]. In addition, self-focusing is generated because of the phenomenon [3], which may damage the laser media and limit the laser outpower. Thus, ways to improve the beam uniformity by smoothing the intensity distributions of laser pulse has became an interesting topic and has been the subject of many investigations in the last decades [4–17]. To achieve beam smoothing, some techniques have been studied, such as using soft-edged aperture [4], adopting multiple spatial filters [5], converting a coherent wave to a random-phased wave [6], and using a lens array [7]. In addition, the technique of smoothing by spectral dispersion (SSD) of the laser pulse was developed [8]. Following the study, much work was undertaken to develop this technique [9–16] and it evolved into three-dimensional SSD [14]. The applications of the methods investigated in the previous works are effective in improving the beam uniformity and they have been applied extensively, especially the SSD [16].

Also, the beam uniformity can be improved by increasing the bandwidth of the laser pulse [17]. When the broadband laser pulse is adopted in the highpower laser system, the uniform illumination of the targets is improved in the high-power laser driver, and some benefits such as eliminating

* Corresponding author. Tel.: +86 21 69918809; fax: +86 21 69918800.
E-mail addresses: pengrunwu@siom.ac.cn, pengrunwu@163.com (R. Peng).

0030-4018/$ - see front matter © 2005 Elsevier B.V. All rights reserved.
doi:10.1016/j.optcom.2005.09.047

the diffraction and the interference effects, weakening optical noise and decreasing the self-focusing are generated for laser system itself. However, the laser pulse investigated in [17] is transform-limited pulse and the increase of the bandwidth is achieved by decreasing the pulse duration. Generally, the broadband laser pulse is generated by broadening the femtosecond or piecosecond pulse to nanosecond pulse in the high-power laser system, and thus the pulse takes big frequency chirp, in which the chirp parameter reaches 10^3–10^4 and even bigger. To know and utilize such big-frequency chirped Gaussian pulse better, it is necessary to study the properties of the pulse.

In the present paper, we have studied the effect of the frequency chirp on the intensity distributions of the chirped Gaussian pulse passing through a hard-edged aperture. In Section 2, the propagation expression of a chirped Gaussian pulse passing through a hard-edged aperture is derived firstly. Then the time-integrated intensity distributions in the pulse with Gaussian transverse profile in the near and far fields are analyzed by numerical calculations in Section 3. In addition, we also investigated the smoothing effect in the pulse with Hermite–Gaussian transverse profile in Section 4. Finally, a brief summary of the results concludes the paper in Section 5.

2. Fields of the chirped Gaussian pulse passing through a hard-edged aperture

The scalar Fresnel–Kirchhoff diffraction integral is obtained from the Helmholtz equation by using the Green's theorem and the Kirchhoff's boundary conditions. When the distance between the examined plane and the aperture is greater than the half width of the aperture, the Fresnel–Kirchhoff diffraction integral is deduced to Huygens–Fresnel diffraction integral [18,19]. Thus, when a laser pulse passes through a hard-edged aperture, we obtain the field in the frequency domain in terms of the Huygens–Fresnel diffraction integral as

$$\tilde{E}(x,z,\omega) = \left(\frac{\mathrm{i}}{\lambda z}\right)^{1/2} \exp(-\mathrm{i}kz) \int_{-a}^{a} \tilde{E}(x_0,0,\omega) \times \exp\left[-\frac{\mathrm{i}k}{2z}(x_0-x)^2\right] \mathrm{d}x_0, \tag{1}$$

where $k = \omega/c$ is wave number, a is half width of the hard-edged aperture, and

$$\tilde{E}(x_0,0,\omega) = \frac{1}{(2\pi)^{1/2}} \int_{-\infty}^{\infty} E(x_0,0,t) \exp(-\mathrm{i}\omega t)\, \mathrm{d}t \tag{2}$$

is field of the incident pulse in the frequency domain and $E(x_0,0,t)$ is field of the incident pulse in the time domain. Assuming the space and time field of the initial pulse can be separated, thus $E(x_0,0,t)$ can be written as

$$E(x_0,0,t) = E(x_0,0) f(t), \tag{3}$$

where $E(x_0,0)$ is the spatial form of the pulse at $z=0$ and $f(t)$ is the field distribution at $x=z=0$ in time domain. It should be pointed that we adopt the assumption in Eq. (3) not because it is very realistic but to make easier our evaluations and qualitatively similar results would be obtained with more sophisticated models. Thus, Eq. (2) can be rewritten as

$$\tilde{E}(x_0,0,\omega) = E(x_0,0)\tilde{f}(\omega), \tag{4}$$

where

$$\tilde{f}(\omega) = \frac{1}{(2\pi)^{1/2}} \int_{-\infty}^{\infty} f(t) \exp(-\mathrm{i}\omega t)\, \mathrm{d}t. \tag{5}$$

Assume that temporal form of the pulse is a chirped Gaussian shape whose field at $z=0$ is in the form

$$f(t) = \exp\left(-a_g^2 \frac{t^2}{T_p^2}\right) \exp[\mathrm{i}(\omega_0 t - Ct^2)], \tag{6}$$

where $a_g = (2\ln 2)^{1/2}$, T_p is pulse duration (full-width at half-maximum, FWHM), ω_0 is the carrier frequency, C is the chirp parameter, and the initial phase φ is omitted. By substituting Eq. (6) into Eq. (5), spectrum $\tilde{f}(\omega)$ at $z=0$ is expressed as

$$\tilde{f}(\omega) = \left[\frac{\pi T_p^2}{a_g^2(1+\mathrm{i}C)}\right]^{1/2} \exp\left[-\frac{T_p^2(\omega-\omega_0)^2}{4a_g^2(1+\mathrm{i}C)}\right]. \tag{7}$$

The field of any point behind the hard-edged aperture in time domain is derived from inverse Fourier transform of Eq. (1) as

$$E(x,z,t) = \frac{1}{(2\pi)^{1/2}} \int_{-\infty}^{\infty} \tilde{E}(x,z,\omega) \exp(\mathrm{i}\omega t)\, \mathrm{d}\omega. \tag{8}$$

In the highpower laser system, the time-integrated intensity (energy density) of the laser pulse was paid more attention, which is obtained as

$$I_{\text{time-integrated}}(x,z) = \int_{-T_p}^{T_p} |E(x,z,t)|^2\, \mathrm{d}t. \tag{9}$$

3. Effects of frequency chirp on the fields of the pulse with Gaussian transverse profile

Consider that the spatial form of the pulse in Eq. (3) is Gaussian transverse profile whose beam width is located at the aperture plane, which is expressed as

$$E(x_0,0) = \exp\left(-\frac{x_0^2}{w_0^2}\right), \tag{10}$$

where w_0 is the waist width of the Gaussian transverse profile and the constant A_0 is omitted.

The integral calculation of Eq. (1) yields

$$\tilde{E}_0(x,z,\omega) = \left[\frac{\mathrm{i}z_R}{4(z+\mathrm{i}z_R)}\right]^{1/2} \exp(-\mathrm{i}kz) \exp\left[-\frac{\mathrm{i}kx^2}{2(z+\mathrm{i}z_R)}\right] \times [\mathrm{erf}(\chi_+) + \mathrm{erf}(\chi_-)]\tilde{f}(\omega), \tag{11}$$

where

$$\chi_+ = \left[\frac{k(z+\mathrm{i}z_\mathrm{R})}{2zz_\mathrm{R}}\right]^{1/2}\left(a+\frac{\mathrm{i}z_\mathrm{R}x}{z+\mathrm{i}z_\mathrm{R}}\right), \tag{12}$$

$$\chi_- = \left[\frac{k(z+\mathrm{i}z_\mathrm{R})}{2zz_\mathrm{R}}\right]^{1/2}\left(a-\frac{\mathrm{i}z_\mathrm{R}x}{z+\mathrm{i}z_\mathrm{R}}\right) \tag{13}$$

and

$$\mathrm{erf}(y) = \frac{2}{\pi^{1/2}}\int_0^y \exp(-x^2)\,\mathrm{d}x \tag{14}$$

is error function. Thus, the field distribution in time domain is given by

$$E_0(x,z,t) = \left[\frac{\mathrm{i}z_\mathrm{R}}{8\pi(z+\mathrm{i}z_\mathrm{R})}\right]^{1/2}\int_{-\infty}^{\infty}[\mathrm{erf}(\chi_+)+\mathrm{erf}(\chi_-)] \times\left[\frac{\pi T_\mathrm{p}^2}{a_\mathrm{g}^2(1+\mathrm{i}C)}\right]^{1/2}\exp\left[-\frac{T_\mathrm{p}^2(\omega-\omega_0)^2}{4a_\mathrm{g}^2(1+\mathrm{i}C)}\right] \times\exp(\mathrm{i}\omega\tau')\,\mathrm{d}\omega, \tag{15}$$

where

$$\tau' = \tau - \frac{x^2}{2c(z+\mathrm{i}z_\mathrm{R})}, \tag{16}$$

$\tau = t - z/c$ is the local time. The time-integrated intensity (energy density) of the beam is given by Eq. (9).

Using the above expressions, we analyzed the effects of the frequency chirp on the fields of the pulse with Gaussian transverse profile by numerical illustrations as follows. In fact, the effect of the frequency chirp on the intensity is the effect of the spectrum broadened by the frequency chirp. When the chirp parameter C is given in the chirped Gaussian pulse, the width of the spectrum is obtained as

$$\Delta\omega = \frac{2a_\mathrm{g}^2(1+C^2)^{1/2}}{T_\mathrm{p}} \tag{17}$$

and thus the bandwidth $\Delta\lambda$ is also obtained relatively. The chirp parameters in the following calculations are $C = 100$, 5000, and 10,000, and thus $\Delta\lambda$ are 0.2, 10, and 20 nm, relatively, where the calculation parameters are $\lambda_0 = 800$ nm and $T_\mathrm{p} = 0.47$ ns, and $a = 1$ mm additionally. The time-integrated intensity distributions in the pulse with Gaussian transverse profile at $z = 5$ mm are given in Fig. 1. It can be seen that many intensity peaks are generated because of the modulation of the aperture and the amplitude of the intensity peaks in the pulse with $C = 100$ is the greatest in the pulse with $C = 100$, 5000, and 10,000. The amplitude of the peaks of the pulse with $C = 5000$ and 10,000 decreases in the region near the z-axis ($x = 0$) obviously and the intensity uniformity of them are improved. Especially, the intensity uniformity in the pulse with $C = 10{,}000$ is the best in them in the region. However, many peaks with great amplitude still exist at the edge of the intensity distributions and the amplitudes have no significant changes. As pointed in [4], they can be eliminated when soft aperture is adopted in the optical systems.

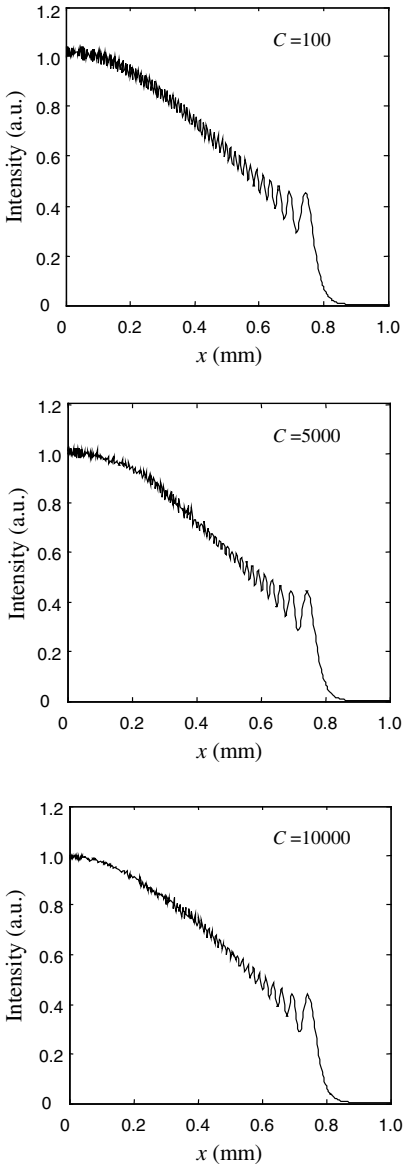

Fig. 1. Time-integrated intensity distributions in the pulse with Gaussian transverse profile at $z = 5$ mm.

The intensity studied in [8] was smoothed in time by overlapping many copies of the pattern, each shifted in space, so that peaks of some fill in the valleys of others and the beam smoothing was achieved. However, the beam smoothing brought by increasing the frequency chirp studied in this paper results from different extent of diffraction of each frequency component physically. We know that the diffraction patterns are determined by Fresnel number $F = a^2/\lambda z$, and there exist different Fresnel numbers and thus different diffraction pattern is generated for each frequency component at a determined point. The different diffraction patterns of the frequency components differ from one another in spatial distribution and the intensity peaks of some fill in the intensity valleys of others when the

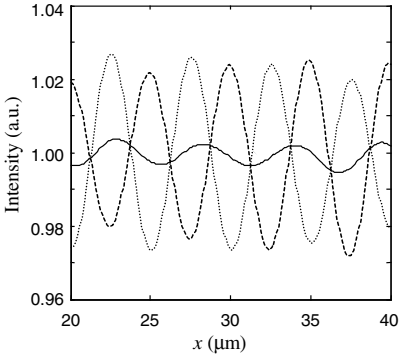

Fig. 2. Intensity distributions of waves of wavelengths 798 and 802 nm with Gaussian transverse profile and the overlapped intensity distribution of them at $z = 5$ mm. The solid line is the overlapped intensity distribution; the dashed line is the intensity distribution of wave with wavelength 798 nm; the dot line is the intensity distribution of wave with wavelength 802 nm.

diffraction patterns of all frequency components are overlapped, so that the intensity is smoothed. Fig. 2 gives the intensity distributions of waves of wavelengths 798 and 802 nm with Gaussian transverse profile and the overlapped intensity distribution of them at $z = 5$ mm. The intensity peaks and the intensity valleys of the two waves are staggered in the region depicted in the figure, so that the peaks fill in the valleys, which results in the smoothing of the overlapped intensity. The bigger the frequency chirp, the larger the bandwidth and the more phenomenon that the peaks fill in the valleys is generated, and thus the better the smoothing effect is achieved.

The time-integrated intensity distributions in the pulse with Gaussian transverse profile at $z = 10$ m are depicted in Fig. 3, from which it can be seen that there is no any intensity peaks are generated in the intensity distributions in the far field. In the transform-limited pulse, the radius of time-integrated intensity distributions tends to decrease with increasing the frequency chirp in the far field [17]. However, the tendency is also exist but unnoticeable in the chirped Gaussian pulse, and the time-integrated intensity distributions in the pulse with different frequency chirp seems to be the same.

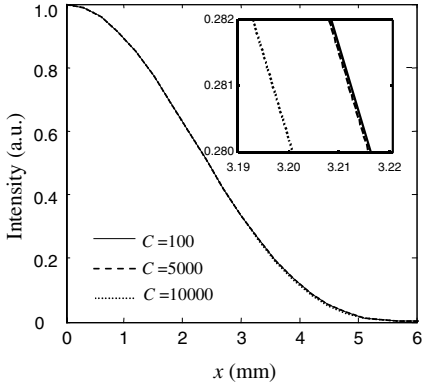

Fig. 3. Time-integrated intensity distributions in the pulse with Gaussian transverse profile at $z = 10$ m.

4. Effects of frequency chirp on the fields of the pulse with Hermite–Gaussian transverse profile

Consider that the spatial form of the pulse in Eq. (3) is a higher-order Gaussian transverse profile whose beam width is also located at the aperture plane. In rectangular coordinates, the higher-order Gaussian transverse profile is in the form of Hermite–Gaussian transverse profile, which is expressed as

$$E_m(x_0, 0) = H_m\left(\sqrt{2}\frac{x_0}{w_0}\right)\exp\left(-\frac{x_0^2}{w_0^2}\right), \tag{18}$$

where $H_m()$ is Hermite polynomial functions and m is mode index. When $m = 0$, Eq. (18) reduces to Eq. (10). When $m = 1$, the integral calculation of Eq. (8) yields

$$\begin{aligned} E_1(x,z,t) = {} & \left[\frac{izz_R}{\pi^2(z+iz_R)^2}\right]^{1/2}\int_{-\infty}^{\infty}\left\{\exp(-\chi_+)^2 - \exp(-\chi_-)^2\right. \\ & \left. + i\sqrt{\frac{\pi k z_R}{2(z+iz_R)}}[\mathrm{erf}(\chi_+) + \mathrm{erf}(\chi_-)]x\right\} \\ & \times\left[\frac{\pi T_p^2}{a_g^2(1+iC)}\right]^{1/2}\exp\left[-\frac{T_p^2(\omega-\omega_0)^2}{4a_g^2(1+iC)}\right] \\ & \times\exp(i\omega\tau')\,d\omega, \end{aligned} \tag{19}$$

and $m = 2$, yields

$$\begin{aligned} E_2(x,z,t) = {} & \left[\frac{iz^2 z_R}{2\pi^2(z+iz_R)^3}\right]^{1/2}\int_{-\infty}^{\infty}\left\{-4\chi_-\exp(-\chi_+)^2\right. \\ & -4\chi_+\exp(-\chi_-)^2 + \sqrt{\pi}\left(1 - \frac{iz_R}{z} - \frac{2kz_R x^2}{(z^2+izz_R)}\right) \\ & \left.\times[\mathrm{erf}(\chi_+) + \mathrm{erf}(\chi_-)]\right\}\left[\frac{\pi T_p^2}{a_g^2(1+iC)}\right]^{1/2} \\ & \times\exp\left[-\frac{T_p^2(\omega-\omega_0)^2}{4a_g^2(1+iC)}\right]\exp(i\omega\tau')\,d\omega. \end{aligned} \tag{20}$$

For other pulses with Hermite–Gaussian transverse profile with higher-order modes, the field expressions can be derived by means of recurrence equations of Hermite polynomials [20,21]. Also, the time-integrated intensity is given by Eq. (9).

Taking the pulse with Hermite–Gaussian transverse profile with $m = 1$ as an example, we studied the effect of the frequency chirp on the time-integrated intensity in the chirped Gaussian pulse with Hermite–Gaussian transverse profile passing through the hard-edged aperture. Fig. 4 gives the time-integrated intensity in the pulse with Hermite–Gaussian transverse profile with $m = 1$ at $z = 5$ mm. It can be seen from the figure that the time-integrated intensity in the pulse on the z-axis is still zero, as well as the continuous wave in the free space [20]. Also, the amplitude of the intensity peaks decreases and the time-integrated intensity in the pulse tends to be smoothed when the frequency chirp increases. Thus, the beam uniformity

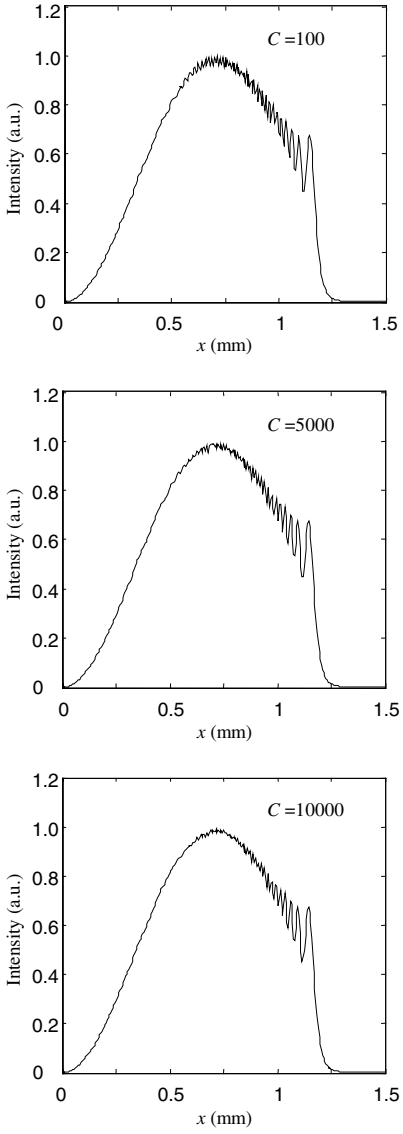

Fig. 4. Time-integrated intensity distributions in the pulse with Hermite–Gaussian transverse profile with $m = 1$ at $z = 5$ mm.

is improved by increasing the frequency chirp in the pulse with Hermite–Gaussian transverse profile as well.

5. Conclusions

Effect of the frequency chirp on the time-integrated intensity distributions of the chirped Gaussian pulse passing through a hard-edged aperture is analyzed in detail. Increasing the frequency chirp in the chirped Gaussian pulse results in increasing the bandwidth of the pulse, which brings a benefit of improving the time-integrated intensity uniformity in the practical applications. The benefit is caused by that the different diffraction patterns are generated because of different extent of diffraction of each frequency component and the intensity peaks of some fill in the intensity valleys of others when the diffraction patterns of all frequency components are overlapped, so that the intensity is smoothed. The results show that the beam smoothing is achieved both in the pulse with Gaussian transverse profile and that with Hermite–Gaussian transverse profile by increasing the frequency chirp.

The bandwidth of the laser pulse already reaches 20 nm in the design of high-power laser driver at present. The beam smoothing is achieved to a certain degree in the pulse with bandwidth 20 nm, but the smoothing effect is not good enough in the laser applications. Due to limitation of some factors, it is very difficult to increase the bandwidth in such high-power laser system further. To obtain more uniform intensity in high-power laser system, it is necessary to combine the other method with the broadband laser pulse. For example, when a dispersive wedge is adopted in the broadband laser pulse, the different diffraction patterns generated by the frequency components will stagger an appropriate distance, which is of more advantage to the fill of the intensity peaks in the intensity valleys, so that better smoothing effect is achieved. It is a subject worthy of study.

Acknowledgments

This work is partially supported by the National Natural Science Foundation of China (Grant Nos. 10576012 and 60538010) and the Specialized Research Fund for the Doctoral Program of Higher Education of China (Grant No. 20040532005).

References

[1] K.A. Bruecker, S. Jorna, Rev. Mod. Phys. 46 (1974) 325.
[2] S. Skupsky, K. Lee, J. Appl. Phys. 54 (1983) 3662.
[3] P.L. Kelly, Phys. Rev. Lett. 15 (1965) 1005.
[4] V.R. Cositich, B.C. Johnson, Laser Focus 10 (1974) 43.
[5] J.T. Hunt, P.A. Renard, W.W. Simmons, Appl. Opt. 16 (1977) 779.
[6] Y. Kato, K. Mima, N. Miyanaga, S. Arinaga, Y. Kitagawa, M. Nakatsuka, C. Yamanaka, Phys. Rev. Lett. 53 (1984) 1057.
[7] X.M. Deng, X.C. Liang, Z.Z. Chen, W.Y. Yu, R.Y. Ma, Appl. Opt. 25 (1986) 377.
[8] S. Skupsky, R.W. Short, T. Kessler, R.S. Craxton, S. Letzring, J.M. Soures, J. Appl. Phys. 66 (1989) 3456.
[9] H. Nakano, K. Tsubakimoto, N. Miyanaga, M. Nakatsuka, T. Kanabe, H. Azechi, T. Jitsuno, S. Nakai, J. Appl. Phys. 73 (1993) 2122.
[10] I. Matsushima, T. Tomie, Y. Matsumoto, I. Okuda, E. Miura, H. Yashiro, E. Takahashi, Y. Owadano, Opt. Commun. 120 (1995) 299.
[11] J.E. Rothenberg, J. Opt. Soc. Am. B 14 (1997) 1664.
[12] H.A. Rose, S. Ghosal, Phys. Plasmas 5 (1998) 775.
[13] Q.F. Tan, Y.B. Yan, G.F. Jin, M.X. Wu, Opt. Commun. 189 (2001) 167.
[14] G. Miyaji, N. Miyanaga, S. Urushihara, K. Suzuki, S. Matsuoka, M. Nakatsuka, A. Morimoto, T. Kobayashi, Opt. Lett. 27 (2002) 725.
[15] Q.F. Tan, Y.B. Yan, G.F. Jin, Opt. Express 12 (2004) 3270.
[16] LLE Review 69 (1996) 1.
[17] R.W. Peng, Y.X. Ye, Z.X. Tang, D.Y. Fan, J. Opt. Soc. Am. A 22 (2005) 1903.
[18] M. Born, E. Wolf, Principles of Optics, seventh ed., Cambridge University Press, Cambridge, 1999.
[19] F. Lytle, Appl. Spectrosc. 53 (1999) 212A.
[20] A.E. Siegman, Lasers, University Science Books Press, CA, 1986.
[21] B.D. Lu, R.W. Peng, Opt. Laser Technol. 35 (2003) 435.